Matta, JM., Ashby, MC., Sanz-Clemente, A., Roche, KW., & Isaac, JT. (2011). mGluR5 and NMDA receptors drive the experience- and activity-dependent NMDA receptor NR2B to NR2A subunit switch. *Neuron*, *70*(2), 339 - 351. https://doi.org/10.1016/j.neuron.2011.02.045

Published in final edited form as:
Neuron. 2011 April 28; 70(2): 339–351. doi:10.1016/j.neuron.2011.02.045.

mGluR5 and NMDA Receptors Drive the Experience- and Activity-Dependent NMDA Receptor NR2B to NR2A Subunit Switch

Jose A. Matta[1,*], **Michael C. Ashby**[1], **Antonio Sanz-Clemente**[2], **Katherine W. Roche**[2], and **John T. R. Isaac**[1,*,+]

[1]Developmental Synaptic Plasticity Section, National Institute of Neurological Disorders and Stroke, National Institutes of Health, Bethesda, MD20892, USA

[2]Receptor Biology Section, National Institute of Neurological Disorders and Stroke, National Institutes of Health, Bethesda, MD20892, USA

Summary

In cerebral cortex there is a developmental switch from NR2B- to NR2A-containing NMDA receptors (NMDARs) driven by activity and sensory experience. This subunit switch alters NMDAR function, influences synaptic plasticity, and its dysregulation is associated with neurological disorders. However, the mechanisms driving the subunit switch are not known. Here we show in hippocampal CA1 pyramidal neurons that the NR2B- to NR2A switch driven acutely by activity requires activation of NMDARs and mGluR5, involves PLC, Ca^{2+} release from IP_3R-dependent stores and PKC activity. In mGluR5 knock-out mice the developmental NR2B-NR2A switch in CA1 is deficient. Moreover, in visual cortex of mGluR5 knock-out mice the NR2B-NR2A switch evoked in vivo by visual experience is absent. Thus we establish that mGluR5 and NMDARs are required for the activity-dependent NR2B-NR2A switch and play a critical role in experience-dependent regulation of NMDAR subunit composition in vivo.

INTRODUCTION

The NMDA receptor (NMDAR) is a ligand-gated ion channel permeable to Na^+, K^+ and Ca^{2+}, and is found at excitatory synapses throughout the brain. NMDARs are required for many forms of learning and memory, and are implicated in numerous neurological disorders (Cull-Candy et al., 2001). Glutamate is the major excitatory neurotransmitter in the brain; it serves as the ligand for NMDARs and receptor activation requires glutamate binding and membrane depolarization. Such coincidence detection and calcium permeability enables the NMDAR to play a pivotal role in synaptic function and plasticity (Bliss and Collingridge, 1993). NMDARs are heterotetramers composed of two NR1 subunits and two NR2 subunits. Most of the diversity in the single channel and pharmacological properties of NMDARs arises from the NR2 subunit composition of the receptor (Cull-Candy et al., 2001).

NMDAR subunit composition varies between different brain regions and throughout development (Monyer et al., 1994; Cull-Candy et al., 2001) In cerebral cortex there is a

[*]Correspondence: mattaja@mail.nih.gov, isaacjo@lilly.com .
[+]Present address: Eli Lilly and Company, Windlesham, Surrey, GU20 6PH, UK.

ubiquitous regulation of NR2 subunit composition during development in which NR2B is the major NR2 subunit during the first postnatal week with NR2A expression increasing thereafter (Monyer et al., 1994; Sans et al., 2000; Sheng et al., 1994). NR2B-containing NMDARs exhibit slower kinetics than NR2A-containing receptors (Williams et al., 1993) and are also selectively blocked by ifenprodil and related compounds (Williams, 1993).

Consistent with the expression changes in NR2 subunits, NMDAR currents at cortical synapses exhibit faster decay kinetics and reduced sensitivity to ifenprodil during development (Carmignoto and Vicini, 1992; Hestrin, 1992; Flint et al., 1997; Tovar and Westbrook, 1999; Kirson and Yaari, 1996; Williams et al., 1993) demonstrating that synaptic NMDARs switch from those predominantly containing NR2B to those containing NR2A. The switch in NR2 subunit composition is dependent on neuronal activity and experience. In primary visual cortex the developmental switch requires visual experience (Carmignoto and Vicini, 1992) and in dark-reared animals can be rapidly induced with only 1 hour of exposure to visual experience (Quinlan et al., 1999; Philpot et al., 2001). Moreover, at synapses on hippocampal CA1 pyramidal neurons synaptic activity can drive NR2A subunits into synapses (Barria and Malinow 2002) and LTP induction in the neonate acutely drives the switch of synaptic NMDARs from NR2B- to NR2A-containing (Bellone and Nicoll, 2007). The NR2B to NR2A switch causes important changes to NMDAR function, altering the amount of calcium influx through the pore and the types of proteins interacting with the intracellular domain of the receptor. These features regulate the type of long-term synaptic plasticity (LTP or LTD) that NMDAR activation can induce, although the exact relationship between NR2 subunits and the induction of LTP and LTD remains controversial (Bartlett et al., 2007; Liu et al., 2004; Morishita et al., 2007; Xu et al., 2009).

Despite the ubiquitous nature and critical roles of the NR2B-NR2A switch in cortical synapse function and plasticity during development, the mechanisms for induction of the subunit switch has not been characterized. We now show that the acute activity-dependent subunit switch induced by an LTP induction protocol in hippocampal CA1 pyramidal cells requires activation of both NMDARs and mGluR5. Further we find that a signaling cascade involving PLC activation, release of calcium from IP_3R-dependent stores and PKC activity is required. However, unlike LTP-induced changes in AMPAR function, the activity-dependent switch in NR2 subunit composition does not require CaMKII or PKA activity. Using mGluR5 knock-out mice, we confirm the requirement for mGluR5 in acutely driving the switch in CA1 hippocampus. Further, we show that the mGluR5 knock-out mice have a deficient developmental switch from NR2B- to NR2A-containing receptors at synapses onto hippocampal CA1 pyramidal neurons and onto layer 2/3 pyramidal primary visual cortical neurons. Moreover, the experience-dependent switch from NR2B to NR2A-containing receptors in layer 2/3 visual cortex of dark-reared animals induced by brief (2.5 hours) light exposure is absent in mGluR5 knock-out mice. Thus we define the mechanisms for the activity-dependent switch in NR2 subunit composition at CA1 synapses and further demonstrate a crucial role in vivo for mGluR5 in driving the experience-dependent switch in NR2 subunit composition.

RESULTS

Activity-dependent change in the NMDAR NR2 subunit composition at hippocampal CA1 pyramidal cell synapses

During the first week of postnatal development, most NMDARs at cortical synapses contain NR2B, whereas by the third postnatal week, a change in composition has occurred whereby the majority of receptors now contain NR2A and lack NR2B (Monyer et al., 1994; Sans et al., 2000; Sheng et al., 1994). Previous work shows that a pairing protocol, which induces LTP of AMPAR-mediated synaptic transmission, also causes a switch of NMDAR subunit

composition from NR2B- to NR2A-containing at CA1 synapses in acute hippocampal slices prepared from postnatal day (P)2 - P9 rats (Bellone and Nicoll, 2007). We used this paradigm to investigate the mechanism for the activity-dependent switch in NR2 subunit composition. Using whole-cell patch-clamp recordings from CA1 pyramidal neurons in acute hippocampal slices, we monitored pharmacologically isolated NMDAR-mediated EPSCs (voltage-clamped at a holding potential of +40 mV to relieve voltage-dependent magnesium block on the NMDAR, in the presence of 5 μM NBQX and 50 μM picrotoxin) evoked at two independent Schaffer collateral/commissural inputs. Following a baseline period we applied a pairing protocol (1 Hz afferent stimulation for 120 seconds at a holding potential of 0 mV) to one pathway (test path). This induction protocol did not cause a change in NMDA EPSC peak amplitude; however, it did produce a speeding of NMDA EPSC decay in the test path, whereas the control path did not exhibit any change in kinetics (Fig. 1A, B). On average, the weighted time constant (τ_w) for the EPSC decay in the test path was ~ 71 ms faster after the induction protocol compared to before the induction protocol, whereas there was no significant difference in the control path (Fig. 1D). In the same cells we then bath-applied the NR2B selective inhibitor, ifenprodil (5 μM) and found that the NMDA EPSCs in the test path were blocked to a smaller degree than those in the control path (Fig. 1A, C). Across all cells, in the control path, ifenprodil reduced the NMDAR EPSC amplitude to ~ 41% of pre-ifenprodil baseline (immediately prior to ifenprodil application), whereas in the test path, ifenprodil was much less effective, only reducing EPSCs to ~ 76 % of pre-drug amplitude (Fig. 1E). These results confirm previous findings (Bellone and Nicoll, 2007) that synaptic activity rapidly drives a switch in synaptic NMDAR composition from those containing NR2B to NR2A-containing receptors. Moreover, in these experiments application of ifenprodil caused NMDA EPSC kinetics to become faster in the control path; however, in the test path ifenprodil did not cause a speeding of kinetics (Fig. S1). This lack of a significant change in kinetics in the test path after application of ifenprodil reflects the small amount of ifenprodil block at this input. These findings confirm that ifenprodil exerts its action by selectively blocking NR2B-containing NMDARs that mediate the slow kinetics of the EPSC and provides further evidence that such receptors are removed from synapses during LTP.

Previous work suggests that long periods of baseline stimulation can itself induce plasticity of the NMDAR EPSC (Bellone and Nicoll, 2007). Therefore to determine if our baseline stimulation protocol (10 EPSCs evoked at 0.1 Hz) was inducing any plasticity we reduced the baseline to 4 evoked responses per path and then tested whether a similar degree of change in kinetics and ifenprodil sensitivity could be induced by the induction protocol. Under these reduced baseline conditions, we observed a similar degree of change in the NMDAR EPSC decay kinetics and ifenprodil sensitivity produced by the induction protocol as for the previous data set with the longer baseline (Fig. S2). Thus our baseline stimulation protocol itself does not evoke significant activity-dependent changes in NMDAR subunit composition.

The interpretation that NR2B-containing NMDARs are removed from synapses and replaced with NR2A relies on the changes in kinetics and pharmacology of the NMDAR EPSC. However, for this latter assay, ifenoprodil may have actions at targets other than NR2B; therefore, in a separate set of experiments we tested changes in sensitivity to a second NR2B selective antagonist, Ro25-6981. We observed a very similar change in the sensitivity to Ro25-6981 as for ifenprodil following induction of the NMDAR subunit switch (Fig. S3). In addition, we developed a culture model to directly image changes in NR2B and NR2A synaptic localization. At DIV 4, cultured hippocampal neurons were chronically treated with D-AP5 to inhibit the developmental subunit switch. After 10 days, D-AP5 was washed off and the cultures treated with glycine to induce an acute switch in NR2 subunit composition. This treatment caused an increase in surface NR2A localization at

synapses and a concomitant loss of NR2B (Fig. S4). Taken together, these findings provide strong evidence that activity drives a rapid switch from NR2B- to NR2A-containing receptors at synapses on CA1 pyramidal neurons.

The activity-dependent change in NMDAR NR2 subunit composition requires mGluR5 and NMDARs

The activity-dependent switch in NR2 subunit composition is rapid and input specific (Fig. 1; Bellone and Nicoll 2007). However the mechanism for its induction is unknown. To investigate this issue we first tested a role for glutamate receptors. As shown in figure 1, and as reported previously (Bellone and Nicoll 2007), the subunit switch can be induced in the presence of NBQX, excluding a requirement for AMPAR activation in the induction mechanism. We therefore hypothesized that NMDAR and/or mGluR activation is required since both these mechanisms cause a rise in spine free calcium concentration that is typically required for induction of synaptic plasticity. The predominant postsynaptic mGluR subtype at CA1 pyramidal cell synapses is mGluR5; therefore, we applied the induction protocol in the presence of MTEP (10 μM), a selective mGluR5 antagonist (Cosford et al., 2003). MTEP fully blocked the activity-dependent speeding of the NMDA EPSC decay kinetics and reduction in NMDA EPSC ifenprodil sensitivity in the test pathway (Fig. 2A-C, J, K). We also tested whether mGluR1 plays any role in the induction of the switch by testing the effects of LY367385 (100 μM), a selective mGluR1 antagonist (Kingston et al., 1999). However, LY367385 failed to block the activity-induced switch in kinetics or ifenprodil sensitivity (Fig. 2D-F, J, K).

We next addressed a role for NMDARs themselves in the induction of the NR2 subunit composition switch. NMDAR activation requires depolarization to relieve the voltage-dependent Mg^{2+} block to allow current flow through the ion channel. Therefore, we first tested a requirement for postsynaptic depolarization in induction of the NR2 subunit switch. In cells in which the test path was stimulated at 1 Hz while the cell was clamped at −70 mV the induction protocol failed to significantly change the NMDA EPSC decay kinetics (Fig. 2J) or ifenprodil sensitivity (Fig. 2K). In the next set of experiments to specifically address the role of NMDARs, we blocked NMDA EPSCs with D-AP5 (50 μM). Once the blockade was complete, we applied the induction protocol and commenced wash-out of D-AP5 immediately. After 20 minutes of wash-out when NMDA EPSCs had recovered to a stable amplitude, decay kinetics between control and test pathways were compared and then ifenprodil was bath-applied (Fig. 2G). D-AP5 completely prevented the activity-dependent switch in NR2 subunit composition (Fig. 2H-K). In control experiments we also tested whether the inability to induce the NR2 subunit switch was due to the extra 20 minutes delay between the induction protocol and the recording of NMDAR EPSCs. We repeated the experiment in the absence of D-AP5 and waited 20 minutes after the induction protocol before comparing NMDAR EPSCs between the control and test paths. Under these conditions, we still reliably observed the differences in the NMDAR EPSC decay kinetics and ifenprodil sensitivity between the control and test paths (Fig. S5).

Previous work has shown that another form of mGluR5-dependent synaptic plasticity, mGluR LTD, requires new protein translation for its expression (Huber et al., 2000). Therefore, we tested whether the protein synthesis inhibitor cycloheximide (60 μM), applied for 1 hour prior to and during the induction protocol, blocked the switch. In the presence of cycloheximide the induction protocol caused robust changes in the NMDAR EPSC decay kinetics and ifenprodil sensitivity (Fig. 2J & K). Taken together, these findings show that the activity-dependent switch in NMDAR NR2 subunit composition requires co-activation of mGluR5 and NMDARs for its induction, but not mGluR1 or new protein synthesis.

PLC and calcium signaling are required for the activity-dependent switch in the NR2 subunit composition

Activation of either NMDARs or mGluR5 leads to a rise in intracellular calcium. We first confirmed the requirement for a rise in postsynaptic free calcium concentration in the activity-dependent NR2 subunit switch (Bellone and Nicoll 2007) by using the calcium chelator BAPTA (10 mM) in the whole-cell recording solution. Postsynaptic BAPTA prevented the pairing protocol-induced speeding of NMDA EPSC kinetics and reduction in ifenprodil sensitivity (Fig. 3J, K).

Whereas a role for calcium influx through NMDARs in generating increases in postsynaptic free calcium concentration is well established, the role for mGluR5-dependent calcium signaling at spines is not so well characterized. To investigate this issue we used two-photon laser scanning microscopy and calcium imaging of spines in CA1 pyramidal neurons in neonatal hippocampal slices. Pyramidal neurons were co-loaded with a calcium-insensitive dye (Alexa 594) and the calcium-sensitive dye Fluo-5F via a patch electrode. A stimulating electrode placed local to the dendrite of interest was used to evoke minimal EPSCs and a spine was identified that responded with a calcium elevation (Fig. S6A-B). A paired pulse stimulation protocol was employed to more reliably elicit synaptic responses because failure rates are high in response to single shock stimulation when using a minimal stimulation protocol. We then compared the spine calcium transient evoked during baseline and in the presence of MTEP and found that MTEP caused a ~50 % reduction in the spine calcium response (Fig. S6C-E). Thus in these neonatal CA1 pyramidal neurons mGluR5 signaling mediates a significant fraction of the evoked postsynaptic calcium transient.

Glutamate binding to mGluR5 leads to activation of PLC and release of calcium from intracellular stores. To test a possible role for this downstream signaling pathway in driving the NR2 subunit switch, we first investigated whether U73122 (5 μM), an inhibitor of PLC, blocked the induction of the subunit switch. In the presence of bath-applied U73122 the induction protocol failed to cause a speeding of NMDA EPSC decay kinetics or reduction ifenprodil sensitivity (Fig. 3A-C, J, K).

We next tested whether calcium release from intracellular stores is involved in the subunit switch. In a first set of experiments we bath-applied thapsigargin (5 μM), which blocks the SERCA pump and causes a rapid depletion of intracellular calcium stores in neurons. In the presence of thapsigargin the changes in EPSC kinetics and ifenprodil sensitivity were completely blocked (Fig. 3J, K). Since PLC activation leads to synthesis of IP_3, we tested a role for release of calcium from IP_3 sensitive stores using two IP_3 receptor inhibitors, heparin and 2APB. We included heparin (10 mg/mL) in the intracellular solution and in a separate set of experiments we bath-applied 2APB (100 μM), which is membrane-permeable. In both sets of experiments the induction protocol failed to cause a change in NMDA EPSC kinetics or ifenprodil sensitivity (Fig. 3J, K). PLC activity also leads to activation of PKC due to the synthesis of DAG and the rise in free calcium concentration that potentially activates a number of PKC isoforms. Therefore we also tested whether PKC activity is required for the NR2 subunit switch and found that application of the induction protocol in the presence of bath-applied GF109203X (1 μM), a PKC inhibitor, prevented the speeding of the NMDA EPSC kinetics and the change in ifenprodil sensitivity (Fig. 3D-F, J, K). Finally, we also tested a role for PKA and CaMKII, two other kinases known to be involved in synaptic plasticity at CA1 synapses (Malenka and Nicoll, 1999). However, neither inhibition of PKA with H89 (10 μM), nor inhibition of CaMKII with KN93 (10 μM) prevented the activity-dependent change in decay kinetics or ifenprodil sensitivity (Fig. 3G-K). Taken together, these findings show that the activity-dependent switch in NR2 subunit composition requires PLC activity (but not CaMKII or PKA activity), calcium release from postsynaptic IP_3R-dependent intracellular stores and PKC activation.

The activity-dependent and developmental switch in NR2 subunit composition at CA1 synapses is impaired in mGluR5 knock-out mice

Our approach using multiple chemically-unrelated inhibitors to probe numerous steps in the same signaling pathway make it very unlikely that the results we obtain can be explained by off-target effects of the reagents. However, we also used a genetic approach using mGluR5 knock-out mice both to confirm the role for mGluR5 in the activity-dependent NR2 subunit switch and also to study the role of mGluR5 in NMDAR regulation in vivo. However, when we used the pairing protocol as for the rat slice experiments in hippocampal slices from P5-P7 wild type mice, we could not evoke any robust change in NMDA EPSC kinetics or ifenprodil sensitivity (not shown). One possibility is that the ability to induce the activity-dependent switch 'washes out' rapidly in mouse CA1 pyramidal neurons during whole-cell recordings, similar to the wash-out of AMPAR LTP commonly observed in CA1 pyramidal neurons (Malinow and Tsien, 1990). Recent work shows that high frequency stimulation (100 Hz for 6 s) can change ifenprodil sensitivity of NMDAR-mediated transmission at hippocampal CA1 synapses in adolescent rats (Xu et al., 2009). Therefore we tested whether this induction protocol applied to the test pathway prior to obtaining a whole cell recording could induce the NR2 subunit switch in slices from P5-P7 mice. Application of this high frequency stimulation protocol to the test pathway 20-30 minutes prior to commencing whole-cell recording, consistently caused a speeding in the decay of NMDAR EPSCs in the test path and a reduction in ifenprodil sensitivity compared to the control path (Fig. 4A-C, J, K). We next tested whether the activity-dependent switch induction mechanism in mouse shares a similar signaling pathway with rat. The NR2B to NR2A switch was blocked by MTEP, U73122, or AP5 (Fig. 4D-K) demonstrating that, like rat, the induction depends on NMDARs, mGluR5 and PLC activation. Moreover, we also tested the mouse induction protocol in rat hippocampal slices and found that it also robustly evoked changes in NMDAR EPSC kinetics and ifenprodil (Fig. S7).

Next we examined whether the activity-dependent NR2 subunit switch was deficient in mGluR5 knock-out mice. We compared slices from knock-out and heterozygous littermates with the experimenter blind to genotype. In hippocampal slices from heterozygotes the high frequency induction protocol caused a similar speeding of NMDA EPSC decay kinetics and reduction in ifenprodil sensitivity, similar to that observed in wild types (Fig. 5A-C, G, H). However, in slices from the mGluR5 knock-outs, although small variable changes in NMDA EPSC decay and ifenprodil sensitivity occurred in some experiments following the induction protocol, no significant change in either of these parameters was observed (Fig. 5D-H).

If the activity-dependent switch underlies the developmental regulation of NR2B/NR2A in vivo, a prediction is that the mGluR5 knock-out mice should have altered regulation of NR2 subunit composition in vivo during development. We investigated this possibility by comparing kinetics and ifenprodil sensitivity of NMDA EPSCs in mGluR5 knock-out mice and wild type littermates. At P15-18, NMDA EPSCs from CA1 pyramidal cells in wild type exhibited faster kinetics and a less sensitivity to ifenprodil compared to knock-outs (Fig. 6A-D). However, in the knock-outs there was still a considerable speeding in NMDA EPSC kinetics and reduction in ifenprodil sensitivity during development). Therefore, these findings show there is a deficit in the developmental switch from NR2B- to NR2A-containing NMDARs in the mGluR5 knock-out demonstrating a role for mGluR5 in this process. However, our data also show that additional mechanisms can at least partly support the developmental switch in the absence of mGluR5.

Deficient experience-dependent NR2B-NR2A switch in visual cortex of mGluR5 knock-out mice

The developmental switch from NR2B to NR2A-containing NMDARs is particularly prominent in primary sensory cortex where it has been shown to depend upon sensory experience. Particularly well studied is this process in primary visual cortex of rodents where visual experience for as little as one hour has been shown to drive the switch from NR2B to NR2A in dark-reared animals (Philpot et al 2001; Quinlan et al 1999), and such regulation influences metaplasticity and is required for maturation of receptive fields (Cho et al., 2009; Philpot et al., 2003; Philpot et al 2007). To probe the role of mGluR5 in the regulation of NMDAR function in vivo, we tested whether the experience-dependent NR2B-NR2A switch is deficient in primary visual cortex of mGluR5 knock-out mice.

We first determined whether there was a disruption in the developmental switch from NR2B to NR2A in layer 2/3. We made whole-cell patch-clamp recordings from layer 2/3 pyramidal neurons in slices of primary visual cortex and found that NMDA EPSCs elicited by layer 4 stimulation exhibited longer decay times and greater ifenprodil sensitivity in mGluR5 knock-outs compared to wild type (Fig. 6E-H). This indicates a deficiency in the development switch from NR2B to NR2A-containing receptors.

Visual experience in dark-reared rodents causes a rapid switch from NR2B- to NR2A-containing NMDARs at layer 4 inputs onto layer 2/3 pyramidal neurons in primary visual cortex that depends upon NMDAR activation (Philpot et al., 2001; Quinlan et al., 1999). Therefore we next tested whether this experience-dependent plasticity is disrupted in mGluR5 knock-out mice. We dark-reared wild type mice and mGluR5 knock-out littermates from P6 until P17-19, exposed some of these animals to 2.5 hours of light and then investigated the effects on NMDA EPSCs at layer 4 inputs onto layer 2/3 pyramidal cells. In wild-type mice NMDA EPSCs in animals exposed to light (+LE) exhibited faster kinetics and reduced ifenprodil sensitivity compared to mice that didn't receive light exposure (Fig 7A-E). The degree of change in these parameters was very similar to that previously reported (Philpot et al 2001; Quinlan et al 1999) and confirms that even brief exposure to light can drive the switch from NR2B-NR2A in visual cortex. In mGluR5 knock-out mice light exposure failed to produce any significant change in NMDA EPSC kinetics or ifenprodil sensitivity (Fig. 7A-E). It was also noticeable that the dark-reared wild-type and knock-out mice (that were not exposed to light) exhibited very similar NMDA EPSC kinetics and ifenprodil sensitivity indicating that visual experience and mGluR5 are necessary for the developmental change from NR2B to NR2A-containing NMDARs in visual cortex during the first few postnatal weeks.

DISCUSSION

During the first postnatal week, most cortical synapses express NR2B-containing receptors, whereas later in development (>P14), many of these receptors are replaced with NR2A-containing NMDARs. Synaptic activity is involved in regulating this switch, and a role for sensory experience in primary sensory cortex has also been demonstrated; however, the molecular mechanisms driving this ubiquitous NMDAR subtype switch have hitherto been largely unexplored. Here, we find that activation of both mGluR5 and NMDA receptors is required for this switch to occur at synapses on hippocampal CA1 pyramidal neurons. Furthermore, we define a downstream signaling pathway involving PLC activation, release of Ca^{2+} from IP_3R-dependent stores and activation of PKC (see Fig. 8 for model). Using mGluR5 knock-out mice we confirm the requirement for mGluR5 in the acute activity-dependent switch at CA1 synapses. Moreover, the mGluR5 knock-outs show exhibit a deficit in the developmental switch from NR2B to NR2A both at CA1 synapses and at inputs onto layer 2/3 pyramidal neurons in primary visual cortex. Finally we show that the

NR2B-NR2A switch driven by brief visual experience in layer 2/3 pyramidal neurons in dark-reared mice is absent in the mGluR5 knock-out. These findings define the mechanism for the activity-dependent NR2B-NR2A switch and suggest a central role for this mechanism in the development- and experience-dependent regulation of cortical NMDAR NR2 subunit composition.

Activity-dependent changes in NR2B and NR2A subunit composition: roles of mGluR5 and NMDARs

Our results show that an LTP induction protocol increases the relative amount of NR2A at CA1 synapses in an mGluR5 and NMDA receptor-dependent manner in the neonate. Moreover, mGluR5 function plays an important role in the rapid experience-driven switch in NR2 subunit composition in pyramidal cells in layer 2/3 of the V1 cortex. In support of a requirement for mGluR5 and NMDARs in the activity-dependent change in the NR2 subunits, NMDARs are also required for this rapid experience-driven NR2B-NR2A switch in primary visual cortex (Quinlan et al., 1999). Together, these findings indicate that this mechanism may represent a ubiquitous process in the developing brain for the activity-dependent regulation of NMDAR function. This is in addition to the variety of other mechanisms described for the regulation of NMDAR function and trafficking in more mature brain (for reviews see Chen and Roche, 2007; Lau and Zukin, 2007; Yashiro and Philpot, 2008).Whether the developmental regulation of NR2 subunit composition also involves some of the induction and expression mechanisms described in older animals is unclear and will be of interest to study in future work. High-frequency stimulation can also have long-lasting potentiating effects on NMDAR-mediated synaptic transmission in adult CA1 hippocampus (Bashir et al., 1991). Interestingly, this NMDAR LTP is also dependent on mGluR5 and NMDA receptor activation (O'Connor et al., 1994; Jia et al., 1998; Kotecha et al., 2003; Rebola et al., 2008). Recent work shows that such NMDAR LTP also requires membrane fusion and causes a speeding in the kinetics of the NMDA EPSC (Peng et al., 2010). However, in the present study we did not observe significant changes in NMDAR peak amplitudes after the induction protocol suggesting that in the neonate NR2A-containing receptors replace NR2B-containing receptors as opposed to being added to the existing pool of synaptic NMDARs. Consistent with NMDAR replacement in our experiments, NR2B-containing receptors are more mobile and can diffuse to extrasynaptic sites at greater rates than NR2A-containing receptors (Groc et al., 2006; Tovar and Westbrook, 2002), and NMDARs more rapidly internalize early in development (Washbourne et al., 2004; Roche et al., 2001). Ifenprodil is not an effective inhibitor of NR1/NR2A diheteromers or NR1/NR2A/NR2B triheteromers (Hatton and Paoletti, 2005) at the concentrations we used. Therefore, although we cannot be certain of the NMDAR subunit composition after the induction protocol, our data strongly suggest that activity induces a loss of NR1/NR2B diheteromers and their replacement with NR2A subunit-containing receptors. This conclusion is further supported by the speeding of decay kinetics, which indicates incorporation of NR2A subunit-containing receptors because this subunit produces receptors with faster kinetics (Cull-Candy and Leszkiewicz, 2004).

Previous studies have shown that potentiation of NMDAR-mediated transmission requires signaling downstream of mGluR5, including release of Ca^{2+} from IP_3R-sensitive stores, and activation of PLC and PKC (Grosshans et al., 2002; Kotecha et al., 2003; Kwon and Castillo, 2008; Jia et al., 1998). Although the final mechanism driving the insertion of NR2A into synapses is unclear, a recent study shows that the postsynaptic membrane SNARE protein, SNAP-23, regulates NMDAR surface expression at synapses in hippocampal CA1 pyramidal neurons (Suh et al., 2010). We find that the activity-dependent switch in NR2 subunit composition requires a rise in postsynaptic calcium and release of calcium from IP_3R-dependent stores. Moreover, we find that at spines from neonates,

mGluR5 contributes to ~ 50% of calcium transients during synaptic transmission. Thus it is reasonable to speculate that the activity-dependent switch in the NR2 subunit requires a certain threshold amount of calcium provided by both NMDAR and mGluR5 activation. Consistent with a role for IP_3R-dependent store release, previous work shows that at CA1 synapses activity evokes release of calcium from these stores (Ross et al., 2005). Furthermore, there is abundant evidence for the role of PLC and calcium release from IP_3R-dependent stores in various forms of synaptic plasticity e.g. (Choi et al., 2005; Daw et al., 2002; Fernandez de Sevilla et al., 2008; Gartner et al., 2006; Itoh et al., 2001; Taufiq et al., 2005).

Although we have not formally tested whether all the hallmarks of the subunit switching mechanism we describe in the slice also occur in vivo, ours and other findings strongly suggest that this mechanism is used in vivo to drive the switch from NR2B to NR2A-containing NMDARs. We show that the developmental switch in NR2 subunit composition is deficient in hippocampus and visual cortex of mGluR5 knock out mice and that the sensory experience-driven switching of NR2 subunit composition is absent in mGluR5 knock outs. Moreover, previous work also shows that in visual cortex NMDARs are required for the experience-dependent switch in subunit composition (Quinlan et al., 1999). Taken together these findings strongly support the idea that the mechanism we describe for the induction of the activity-dependent switch as studied in hippocampal slices are used in vivo to drive the NR2 subunit switch. However, the possibility remains that additional mechanisms may also contribute in vivo and this may explain the partial switch from NR2B to NR2A that is still observed during development in the mGluR5 knock outs.

Physiological Role

Long term changes in synaptic efficacy are typically dependent on calcium influx through NMDARs into postsynaptic spines. The polarity of these synaptic changes (strengthening for LTP and weakening for LTD) has been proposed to depend on the amount and temporal dynamics of calcium influx, which could be determined by the NR2 subunit composition of NMDARs (Malenka and Bear, 2004; Yang et al., 1999). In addition to calcium dynamics, differences in binding of signaling molecules to the C-terminal tails of NR2A and NR2B (Strack and Colbran, 1998; Barria and Malinow, 2005; Foster et al., 2010) may further define the polarity of synaptic plasticity. Whether NR2B or NR2A favors LTP or LTD, and vice versa, is still a matter of much debate (Bartlett et al., 2007; Liu et al., 2004; Morishita et al., 2007; Xu et al., 2009). However, dysregulation of NR2 subtype expression at synapses impairs hippocampus-dependent learning and memory demonstrating an important role for NR2 subunits in plasticity (Sakimura et al., 1995; Sprengel et al., 1998; von Engelhardt et al., 2008). Sensory experience shapes cortical receptive fields in primary sensory cortex during critical periods in an NMDAR-dependent manner. In the visual cortex, a developmental switch from NR2B- to NR2A-containing receptors coincides with this critical period (Carmignoto and Vicini, 1992). Also, visual experience or deprivation can rapidly increase or decrease the NR2A/2B ratio of synaptic NMDARs in a reversible manner (Philpot et al., 2001; Quinlan et al., 1999). Similarly, whisker trimming during early postnatal development prevents the developmental changes in the NR2 subunit in barrel cortex (Mierau et al., 2004).

The experience-dependent switch from NR2B to NR2A has important physiological consequences. In primary visual cortex, where this has been most well characterized, the NR2B/NR2A ratio regulates the degree of temporal summation of NMDAR-mediated synaptic responses, sets the modification threshold for synaptic plasticity and regulates receptive field maturation (Cho et al., 2009; Philpot et al., 2001; Philpot et al., 2003). Moreover, a number of neurological disorders involve dysregulation of NR2 subunits. Increased NR2B surface expression is observed in Huntington’s Disease (Fan et al., 2007;

Milnerwood et al.), NMDAR hypofunction and altered NR2B/NR2A trafficking is found in mouse models of schizophrenia (Mohn et al., 1999; Tang et al., 2009), Abeta induces internalization of NMDARs in Alzheimer's disease models (Snyder et al., 2005), and there is increased surface-expression of NR2A-containing NMDARs in cocaine addiction (Borgland et al., 2006). Thus understanding the mechanisms of NR2B/NR2A regulation is important because this can give insight into mechanisms underlying important physiological and pathological changes in a number of brain areas and for a number of different paradigms. Our findings now provide the characterization of the novel induction mechanism underlying a physiological regulation of NR2 subunit composition. Our data suggest that this mechanism is widely used in cortical neurons and it will be of great interest in future studies to determine if this mechanism is also involved in pathological changes in NMDAR subunit composition.

Supplementary Material

Refer to Web version on PubMed Central for supplementary material.

Acknowledgments

This work was supported by the National Institute of Neurological Disorders and Stroke Intramural Program. Dr. Matta is supported on a Pharmacology Research Associate fellowship from NIGMS. We are grateful to Chris McBain and members of the McBain and Isaac labs for discussions on this study. We thank Hey Kyoung Lee and Emily Petrus for advice on the visual cortex experiments.

Appendix

Experimental Procedures

Electrophysiology

4-9 day old Wistar rats were anesthetized with isoflurane and then decapitated in accordance with NIH animal care and use guidelines. Transverse hippocampal slices (400 μm thick) were cut in ice cold artificial cerebrospinal fluid (ACSF) containing (mM): 119 NaCl, 2.5 KCl, 2.5 $CaCl_2$, 9 $MgSO_4$, 1 NaH_2PO_4, 26.2 $NaHCO_3$, 11 glucose equilibrated with 95% O_2 and 5% CO_2. Slices were then allowed to recover for at least one hour in ACSF at room temperature (composition as above except for 1.3 mM $MgSO_4$). Whole cell patch clamp recordings were made from visually identified CA1 pyramidal neurons in the presence of 50μM picrotoxin at room temperature. The whole-cell solution contained (mM) 115 $CsMeSO_4$, 20 $CsCl_2$, 10 HEPES, 2.5 $MgCl_2$, 4 NaATP, 0.4 NaGTP, 10 NaCreatine, and 0.6 EGTA (pH 7.2). Preparation of hippocampal and cortical slices from mice was similar except that the ice cold ACSF for cutting was of the following composition (mM): 87 NaCl, 2.5 KCl, 0.5 $CaCl_2$, 25 $NaHCO_3$, 1.25 NaH_2PO_4, 25 glucose, 75 sucrose equilibrated with 95% O_2 and 5% CO_2, slices were then placed at 35 °C for 30 minutes, and then allowed to recover for at least one hour in ACSF at room temperature.

EPSCs were evoked by electrical stimulation of two independent populations of Schaffer collateral/commissural axons using two bipolar stimulating electrodes placed in stratum radiatum of CA1 (0.1 Hz stimulation frequency). The stimulating electrodes were placed on opposite sides from recorded cell from each other. For layer 2/3 pyramidal cell recordings from the visual cortex, the stimulating electrode was placed in layer 4. NMDAR-mediated EPSCs were obtained in the presence of NBQX (5μM) and picrotoxin (50μM) while cells were voltage-clamped at +40 mV. Recordings in which the access resistance changed by more than 10% were discarded and not included in our analysis. Recordings were performed using a Multiclamp 700B patch-clamp amplifier (Axon Instruments, Foster City, CA); signals were filtered at 4 kHz, digitized at 10 Hz and displayed and analyzed on-line using

pClamp 9.2 (Axon Instruments). To drive the activity dependent switch in the subunit composition of synaptic NMDA receptors from rat slices an LTP induction protocol was employed, in which cells were voltage clamped at 0 mV while Schaffer collateral/commissural axons were stimulated at 1Hz for 120 seconds, similar to that previously described (Bellone and Nicoll, 2007). Cells were then voltage-clamped at −70 mV for 5 minutes following LTP induction. Following these 5 minutes, NMDA receptors EPSCs were once again recorded at a holding potential of +40 mV. For mice, the induction protocol (100 Hz for 6 seconds) was employed in the absence of NBQX, and 20-30 minutes prior to obtaining the whole cell configuration. For both rats and mice, the stimulating electrodes for the test and control pathways were alternated to avoid differences in NMDA EPSC due to proximal or distal synapses. Once cell per slice was used. NMDA EPSC decay was fit with a double exponential function using OriginLab software (Northampton, MA) and decay kinetics are expressed as a weighted decay time constant. All receptor antagonists were bath applied at least 20 minutes prior to and during the induction protocol. For kinase inhibitors, slices were preincubated with inhibitors for at least 1hour prior to the induction protocol.

Dark-rearing

For dark-rearing, male and female mice were used. Dark rearing commenced at P6 and mice were raised in complete darkness until P17-P19. For light experience (LE) experiments, dark-reared mice were exposed to 2.5 hours of light.

Statistics

Values are mean ± standard error of the mean (SEM). Statistical significance was tested using a student's t-test. For all experiments in which genotype was the experimental variable, the 'n' was animal. All drugs, except for picrotoxin (Sigma Aldrich) were obtained from Tocris Cookson.

REFERENCES

Barria A, Malinow R. Subunit-specific NMDA receptor trafficking to synapses. Neuron. 2002; 35:345–353. [PubMed: 12160751]

Barria A, Malinow R. NMDA receptor subunit composition controls synaptic plasticity by regulating binding to CaMKII. Neuron. 2005; 48:289–301. [PubMed: 16242409]

Bartlett TE, Bannister NJ, Collett VJ, Dargan SL, Massey PV, Bortolotto ZA, Fitzjohn SM, Bashir ZI, Collingridge GL, Lodge D. Differential roles of NR2A and NR2B-containing NMDA receptors in LTP and LTD in the CA1 region of two-week old rat hippocampus. Neuropharmacology. 2007; 52:60–70. [PubMed: 16904707]

Bashir ZI, Alford S, Davies SN, Randall AD, Collingridge GL. Long-term potentiation of NMDA receptor-mediated synaptic transmission in the hippocampus. Nature. 1991; 349:156–158. [PubMed: 1846031]

Bellone C, Nicoll RA. Rapid bidirectional switching of synaptic NMDA receptors. Neuron. 2007; 55:779–785. [PubMed: 17785184]

Bliss TV, Collingridge GL. A synaptic model of memory: long-term potentiation in the hippocampus. Nature. 1993; 361:31–39. [PubMed: 8421494]

Borgland SL, Taha SA, Sarti F, Fields HL, Bonci A. Orexin A in the VTA is critical for the induction of synaptic plasticity and behavioral sensitization to cocaine. Neuron. 2006; 49:589–601. [PubMed: 16476667]

Carmignoto G, Vicini S. Activity-dependent decrease in NMDA receptor responses during development of the visual cortex. Science. 1992; 258:1007–1011. [PubMed: 1279803]

Chen BS, Roche KW. Regulation of NMDA receptors by phosphorylation. Neuropharmacology. 2007; 53:362–368. [PubMed: 17644144]

Cho KK, Khibnik L, Philpot BD, Bear MF. The ratio of NR2A/B NMDA receptor subunits determines the qualities of ocular dominance plasticity in visual cortex. Proc Natl Acad Sci U S A. 2009; 106:5377–5382. [PubMed: 19276107]

Choi SY, Chang J, Jiang B, Seol GH, Min SS, Han JS, Shin HS, Gallagher M, Kirkwood A. Multiple receptors coupled to phospholipase C gate long-term depression in visual cortex. J Neurosci. 2005; 25:11433–11443. [PubMed: 16339037]

Cosford ND, Tehrani L, Roppe J, Schweiger E, Smith ND, Anderson J, Bristow L, Brodkin J, Jiang X, McDonald I, et al. 3-[(2-Methyl-1,3-thiazol-4-yl)ethynyl]-pyridine: a potent and highly selective metabotropic glutamate subtype 5 receptor antagonist with anxiolytic activity. J Med Chem. 2003; 46:204–206. [PubMed: 12519057]

Cull-Candy S, Brickley S, Farrant M. NMDA receptor subunits: diversity, development and disease. Curr Opin Neurobiol. 2001; 11:327–335. [PubMed: 11399431]

Cull-Candy SG, Leszkiewicz DN. Role of distinct NMDA receptor subtypes at central synapses. Sci STKE. 2004; 2004:re16. [PubMed: 15494561]

Daw MI, Bortolotto ZA, Saulle E, Zaman S, Collingridge GL, Isaac JT. Phosphatidylinositol 3 kinase regulates synapse specificity of hippocampal long-term depression. Nat Neurosci. 2002; 5:835–836. [PubMed: 12161757]

Fan MM, Fernandes HB, Zhang LY, Hayden MR, Raymond LA. Altered NMDA receptor trafficking in a yeast artificial chromosome transgenic mouse model of Huntington's disease. J Neurosci. 2007; 27:3768–3779. [PubMed: 17409241]

Fernandez de Sevilla D, Nunez A, Borde M, Malinow R, Buno W. Cholinergic-mediated IP3-receptor activation induces long-lasting synaptic enhancement in CA1 pyramidal neurons. J Neurosci. 2008; 28:1469–1478. [PubMed: 18256268]

Flint AC, Maisch US, Weishaupt JH, Kriegstein AR, Monyer H. NR2A subunit expression shortens NMDA receptor synaptic currents in developing neocortex. J Neurosci. 1997; 17:2469–2476. [PubMed: 9065507]

Foster KA, McLaughlin N, Edbauer D, Phillips M, Bolton A, Constantine-Paton M, Sheng M. Distinct roles of NR2A and NR2B cytoplasmic tails in long-term potentiation. J Neurosci. 2010; 30:2676–2685. [PubMed: 20164351]

Gartner A, Polnau DG, Staiger V, Sciarretta C, Minichiello L, Thoenen H, Bonhoeffer T, Korte M. Hippocampal long-term potentiation is supported by presynaptic and postsynaptic tyrosine receptor kinase B-mediated phospholipase Cgamma signaling. J Neurosci. 2006; 26:3496–3504. [PubMed: 16571757]

Groc L, Heine M, Cousins SL, Stephenson FA, Lounis B, Cognet L, Choquet D. NMDA receptor surface mobility depends on NR2A-2B subunits. Proc Natl Acad Sci U S A. 2006; 103:18769–18774. [PubMed: 17124177]

Grosshans DR, Clayton DA, Coultrap SJ, Browning MD. LTP leads to rapid surface expression of NMDA but not AMPA receptors in adult rat CA1. Nat Neurosci. 2002; 5:27–33. [PubMed: 11740502]

Hatton CJ, Paoletti P. Modulation of triheteromeric NMDA receptors by N-terminal domain ligands. Neuron. 2005; 46:261–274. [PubMed: 15848804]

Hestrin S. Developmental regulation of NMDA receptor-mediated synaptic currents at a central synapse. Nature. 1992; 357:686–689. [PubMed: 1377360]

Huber KM, Kayser MS, Bear MF. Role for rapid dendritic protein synthesis in hippocampal mGluR-dependent long-term depression. Science. 2000; 288:1254–1257. [PubMed: 10818003]

Itoh S, Ito K, Fujii S, Kaneko K, Kato K, Mikoshiba K, Kato H. Neuronal plasticity in hippocampal mossy fiber-CA3 synapses of mice lacking the inositol-1,4,5-trisphosphate type 1 receptor. Brain Res. 2001; 901:237–246. [PubMed: 11368972]

Jia Z, Lu Y, Henderson J, Taverna F, Romano C, Abramow-Newerly W, Wojtowicz JM, Roder J. Selective abolition of the NMDA component of long-term potentiation in mice lacking mGluR5. Learn Mem. 1998; 5:331–343. [PubMed: 10454358]

Kingston AE, O'Neill MJ, Bond A, Bruno V, Battaglia G, Nicoletti F, Harris JR, Clark BP, Monn JA, Lodge D, Schoepp DD. Neuroprotective actions of novel and potent ligands of group I and group

II metabotropic glutamate receptors. Ann N Y Acad Sci. 1999; 890:438–449. [PubMed: 10668448]

Kirson ED, Yaari Y. Synaptic NMDA receptors in developing mouse hippocampal neurones: functional properties and sensitivity to ifenprodil. J Physiol. 1996; 497(Pt 2):437–455. [PubMed: 8961186]

Kotecha SA, Jackson MF, Al-Mahrouki A, Roder JC, Orser BA, MacDonald JF. Co-stimulation of mGluR5 and N-methyl-D-aspartate receptors is required for potentiation of excitatory synaptic transmission in hippocampal neurons. J Biol Chem. 2003; 278:27742–27749. [PubMed: 12740378]

Kwon HB, Castillo PE. Long-term potentiation selectively expressed by NMDA receptors at hippocampal mossy fiber synapses. Neuron. 2008; 57:108–120. [PubMed: 18184568]

Lau CG, Zukin RS. NMDA receptor trafficking in synaptic plasticity and neuropsychiatric disorders. Nat Rev Neurosci. 2007; 8:413–426. [PubMed: 17514195]

Liu L, Wong TP, Pozza MF, Lingenhoehl K, Wang Y, Sheng M, Auberson YP, Wang YT. Role of NMDA receptor subtypes in governing the direction of hippocampal synaptic plasticity. Science. 2004; 304:1021–1024. [PubMed: 15143284]

Malenka RC, Bear MF. LTP and LTD: an embarrassment of riches. Neuron. 2004; 44:5–21. [PubMed: 15450156]

Malenka RC, Nicoll RA. Long-term potentiation--a decade of progress? Science. 1999; 285:1870–1874. [PubMed: 10489359]

Malinow R, Tsien RW. Presynaptic enhancement shown by whole-cell recordings of long-term potentiation in hippocampal slices. Nature. 1990; 346:177–180. [PubMed: 2164158]

Mierau SB, Meredith RM, Upton AL, Paulsen O. Dissociation of experience-dependent and -independent changes in excitatory synaptic transmission during development of barrel cortex. Proc Natl Acad Sci U S A. 2004; 101:15518–15523. [PubMed: 15492224]

Milnerwood AJ, Gladding CM, Pouladi MA, Kaufman AM, Hines RM, Boyd JD, Ko RW, Vasuta OC, Graham RK, Hayden MR, et al. Early increase in extrasynaptic NMDA receptor signaling and expression contributes to phenotype onset in Huntington's disease mice. Neuron. 2010; 65:178–190. [PubMed: 20152125]

Mohn AR, Gainetdinov RR, Caron MG, Koller BH. Mice with reduced NMDA receptor expression display behaviors related to schizophrenia. Cell. 1999; 98:427–436. [PubMed: 10481908]

Monyer H, Burnashev N, Laurie DJ, Sakmann B, Seeburg PH. Developmental and regional expression in the rat brain and functional properties of four NMDA receptors. Neuron. 1994; 12:529–540. [PubMed: 7512349]

Morishita W, Lu W, Smith GB, Nicoll RA, Bear MF, Malenka RC. Activation of NR2B-containing NMDA receptors is not required for NMDA receptor-dependent long-term depression. Neuropharmacology. 2007; 52:71–76. [PubMed: 16899258]

O'Connor JJ, Rowan MJ, Anwyl R. Long-lasting enhancement of NMDA receptor-mediated synaptic transmission by metabotropic glutamate receptor activation. Nature. 1994; 367:557–559. [PubMed: 7906392]

Peng Y, Zhao J, Gu QH, Chen RQ, Xu Z, Yan JZ, Wang SH, Liu SY, Chen Z, Lu W. Distinct trafficking and expression mechanisms underlie LTP and LTD of NMDA receptor-mediated synaptic responses. Hippocampus. 2010; 20:646–658. [PubMed: 19489005]

Philpot BD, Cho KK, Bear MF. Obligatory role of NR2A for metaplasticity in visual cortex. Neuron. 2007; 53:495–502. [PubMed: 17296552]

Philpot BD, Espinosa JS, Bear MF. Evidence for altered NMDA receptor function as a basis for metaplasticity in visual cortex. J Neurosci. 2003; 23:5583–5588. [PubMed: 12843259]

Philpot BD, Sekhar AK, Shouval HZ, Bear MF. Visual experience and deprivation bidirectionally modify the composition and function of NMDA receptors in visual cortex. Neuron. 2001; 29:157–169. [PubMed: 11182088]

Quinlan EM, Philpot BD, Huganir RL, Bear MF. Rapid, experience-dependent expression of synaptic NMDA receptors in visual cortex in vivo. Nat Neurosci. 1999; 2:352–357. [PubMed: 10204542]

Rebola N, Lujan R, Cunha RA, Mulle C. Adenosine A2A receptors are essential for long-term potentiation of NMDA-EPSCs at hippocampal mossy fiber synapses. Neuron. 2008; 57:121–134. [PubMed: 18184569]

Roche KW, Standley S, McCallum J, Dune Ly C, Ehlers MD, Wenthold RJ. Molecular determinants of NMDA receptor internalization. Nat Neurosci. 2001; 4:794–802. [PubMed: 11477425]

Ross WN, Nakamura T, Watanabe S, Larkum M, Lasser-Ross N. Synaptically activated ca2+ release from internal stores in CNS neurons. Cell Mol Neurobiol. 2005; 25:283–295. [PubMed: 16047542]

Sakimura K, Kutsuwada T, Ito I, Manabe T, Takayama C, Kushiya E, Yagi T, Aizawa S, Inoue Y, Sugiyama H, et al. Reduced hippocampal LTP and spatial learning in mice lacking NMDA receptor epsilon 1 subunit. Nature. 1995; 373:151–155. [PubMed: 7816096]

Sans NA, Montcouquiol ME, Raymond J. Postnatal developmental changes in AMPA and NMDA receptors in the rat vestibular nuclei. Brain Res Dev Brain Res. 2000; 123:41–52.

Sheng M, Cummings J, Roldan LA, Jan YN, Jan LY. Changing subunit composition of heteromeric NMDA receptors during development of rat cortex. Nature. 1994; 368:144–147. [PubMed: 8139656]

Snyder EM, Nong Y, Almeida CG, Paul S, Moran T, Choi EY, Nairn AC, Salter MW, Lombroso PJ, Gouras GK, Greengard P. Regulation of NMDA receptor trafficking by amyloid-beta. Nat Neurosci. 2005; 8:1051–1058. [PubMed: 16025111]

Sprengel R, Suchanek B, Amico C, Brusa R, Burnashev N, Rozov A, Hvalby O, Jensen V, Paulsen O, Andersen P, et al. Importance of the intracellular domain of NR2 subunits for NMDA receptor function in vivo. Cell. 1998; 92:279–289. [PubMed: 9458051]

Strack S, Colbran RJ. Autophosphorylation-dependent targeting of calcium/calmodulin-dependent protein kinase II by the NR2B subunit of the N-methyl- D-aspartate receptor. J Biol Chem. 1998; 273:20689–20692. [PubMed: 9694809]

Suh YH, Terashima A, Petralia RS, Wenthold RJ, Isaac JT, Roche KW, Roche PA. A neuronal role for SNAP-23 in postsynaptic glutamate receptor trafficking. Nat Neurosci. 2010; 13:338–343. [PubMed: 20118925]

Tang TT, Yang F, Chen BS, Lu Y, Ji Y, Roche KW, Lu B. Dysbindin regulates hippocampal LTP by controlling NMDA receptor surface expression. Proc Natl Acad Sci U S A. 2009; 106:21395–21400. [PubMed: 19955431]

Taufiq AM, Fujii S, Yamazaki Y, Sasaki H, Kaneko K, Li J, Kato H, Mikoshiba K. Involvement of IP3 receptors in LTP and LTD induction in guinea pig hippocampal CA1 neurons. Learn Mem. 2005; 12:594–600. [PubMed: 16287718]

Tovar KR, Westbrook GL. The incorporation of NMDA receptors with a distinct subunit composition at nascent hippocampal synapses in vitro. J Neurosci. 1999; 19:4180–4188. [PubMed: 10234045]

Tovar KR, Westbrook GL. Mobile NMDA receptors at hippocampal synapses. Neuron. 2002; 34:255–264. [PubMed: 11970867]

von Engelhardt J, Doganci B, Jensen V, Hvalby O, Gongrich C, Taylor A, Barkus C, Sanderson DJ, Rawlins JN, Seeburg PH, et al. Contribution of hippocampal and extra-hippocampal NR2B-containing NMDA receptors to performance on spatial learning tasks. Neuron. 2008; 60:846–860. [PubMed: 19081379]

Washbourne P, Liu XB, Jones EG, McAllister AK. Cycling of NMDA receptors during trafficking in neurons before synapse formation. J Neurosci. 2004; 24:8253–8264. [PubMed: 15385609]

Williams K. Ifenprodil discriminates subtypes of the N-methyl-D-aspartate receptor: selectivity and mechanisms at recombinant heteromeric receptors. Mol Pharmacol. 1993; 44:851–859. [PubMed: 7901753]

Williams K, Russell SL, Shen YM, Molinoff PB. Developmental switch in the expression of NMDA receptors occurs in vivo and in vitro. Neuron. 1993; 10:267–278. [PubMed: 8439412]

Xu Z, Chen RQ, Gu QH, Yan JZ, Wang SH, Liu SY, Lu W. Metaplastic regulation of long-term potentiation/long-term depression threshold by activity-dependent changes of NR2A/NR2B ratio. J Neurosci. 2009; 29:8764–8773. [PubMed: 19587283]

Yang SN, Tang YG, Zucker RS. Selective induction of LTP and LTD by postsynaptic [Ca2+]i elevation. J Neurophysiol. 1999; 81:781–787. [PubMed: 10036277]

Yashiro K, Philpot BD. Regulation of NMDA receptor subunit expression and its implications for LTD, LTP, and metaplasticity. Neuropharmacology. 2008; 55:1081–1094. [PubMed: 18755202]

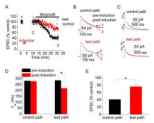

Figure 1. Activity-dependent switch from NR2B- to NR2A-containing NMDARs at hippocampal CA1 pyramidal cell synapses

(A) Summary data of NMDA EPSC peak amplitude vs. time plot for two independent pathways onto the same cell. In one pathway (test; red) the induction protocol was applied, ifenprodil (5 μM) was bath-applied at the time indicated. (B) NMDA EPSCs from example experiments for the test and control pathways taken at the times indicated in A. For this and the other figures, NMDA EPSCs typically didn't exhibit any change in peak amplitude after the induction protocol and so are shown superimposed with no amplitude rescaling. (C) NMDA EPSCs from an example experiment showing changes in the ifenprodil sensitivity in the control and test paths after application of the induction protocol. (D) Summary graph showing the average values for the weighted time constant (τ_w) in the control and test paths, before and after the induction protocol (control path: pre-induction = 282 ± 23 ms, post-induction = 277 ± 22 ms; test path: pre-induction = 285 ± 22 ms, post-induction = 218 ± 16 ms). (E) Summary graph for EPSC amplitude in the presence of ifenprodil expressed as percentage of pre-ifenprodil amplitude (control path = 41 ± 4.1 %; test path = 76 ± 6.2 %). n = 15 cells throughout; slices prepared from P5-7 rat; * indicates $P < 0.05$.

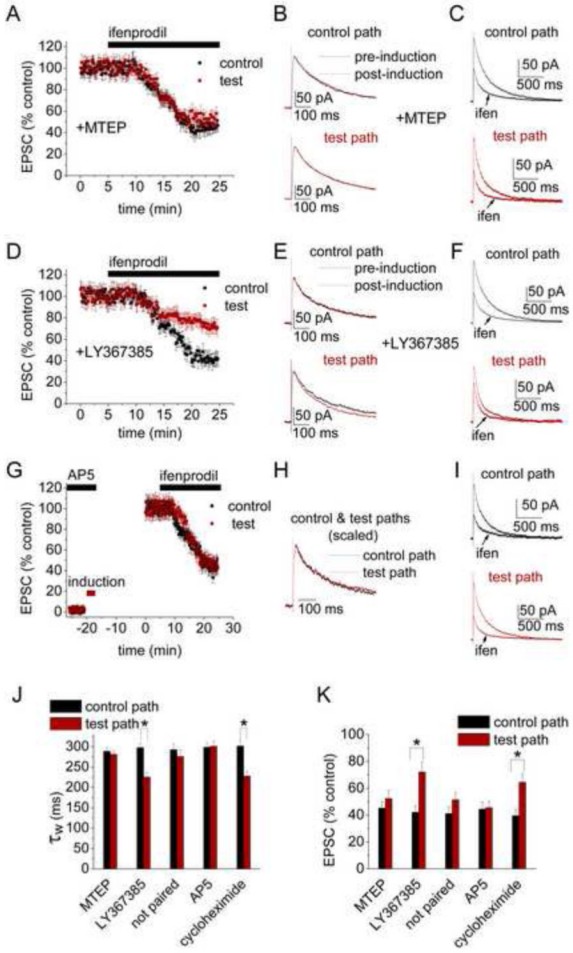

Figure 2. mGluR5 and NMDAR activation are required for the activity-dependent switch in NR2 subunit composition

(A) Summary data of NMDA EPSC peak amplitude vs. time plot for two independent pathways onto the same cell performed in the presence of bath-applied MTEP (10 μM). In one pathway (test; red) the induction protocol was applied, ifenprodil (5 μM) was bath-applied at the time indicated (n = 10). (B) NMDA EPSCs from example experiments for the test and control pathways taken from the experiments in A. (C) NMDA EPSCs from an example experiment showing changes in the ifenprodil sensitivity in the control and test paths after application of the induction protocol. (D-F) As for A-C, but in the presence of LY367385 (100 μM; n = 7). (G-I) As for A-C, but in the presence of D-AP5 (50 μM; n = 8). (J) Summary graph showing the average values for the weighted time constant (τ_w) in the control and test paths, before and after the induction protocol in the presence of the different antagonists (control path: MTEP = 289 ± 8.2 ms, LY367385 = 298 ± 10.5 ms, not paired = 293 ± 14.3 ms, AP5 = 299 ± 11.2 ms, cycloheximide = 302 ± 13.5 ms; test path: MTEP = 282 ± 9.1 ms, LY367385 = 225 ± 11.8 ms, not paired = 276 ± 16.5 ms, AP5 = 302 ± 13.1 ms, cycloheximide = 228 ± 11.5 ms). (K) Summary graph for EPSC amplitude in the presence of ifenprodil expressed as percentage of pre-ifenprodil amplitude in the presence of the different antagonists (control path: MTEP = 45.2 ± 5.1 %, LY367385 = 42.1 ± 4.9 %, not paired = 41.1 ± 4.8 %, AP5 = 44.4 ± 5.2 %, cycloheximide = 39.5 ± 4.8 %; test path: MTEP = 52.3 ± 6.0 %, LY367385 = 72.1 ± 7.5 %, not paired = 51.5 ± 5.3 %, AP5 = 45.6 ± 4.5 %, cycloheximide = 64.5 ± 6.1 %).

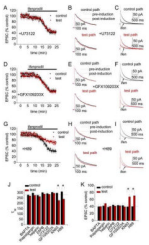

Figure 3. Signaling requirements for the activity-dependent switch in NR2 subunit composition

(A) Summary data of NMDA EPSC peak amplitude vs. time plot for two independent pathways onto the same cell performed in the presence of bath-applied U73122 (5 μM). In one pathway (test; red) the induction protocol was applied, ifenprodil (5 μM) was bath-applied at the time indicated (n = 6). (B) NMDA EPSCs from example experiments for the test and control pathways taken from the experiments in A. (C) NMDA EPSCs from an example experiment showing changes in the ifenprodil sensitivity in the control and test paths after application of the induction protocol. (D-F) As for A-C, but in the presence of GFX109203 (1 μM; n = 8). (G-I) As for A-C, but in the presence of H89 (10 μM; n = 6) (J) Summary graph showing the average values for the weighted time constant (τ_w) in the control and test paths, before and after the induction protocol in the presence of a number of different antagonists (control path: BAPTA = 280 ± 12 ms, thapsigargin = 298 ± 14 ms, heparin = 278 ± 13 ms, 2APB = 302 ± 11 ms, U73122 = 293 ± 14 ms, GF109203X = 305 ± 10 ms, KN93 = 298 ± 11 ms, H89 = 311 ± 14 ms; test path: BAPTA = 271 ± 9 ms, thapsigargin = 276 ± 16 ms, heparin = 265 ± 14 ms, 2APB = 289 ± 13 ms, U73122 = 286 ± 14 ms, GF109203X = 296 ± 13 ms, KN93 = 228 ± 14 ms, H89 = 241 ± 12 ms). (K) Summary graph for EPSC amplitude in the presence of ifenprodil expressed as percentage of pre-ifenprodil amplitude in the presence of the different antagonists (control path: BAPTA = 39.8 ± 6.2 %, thapsigargin = 42.1 ± 7.9 %, heparin = 38.6 ± 4.3 %, 2APB = 44.9 ± 6.7%, U73122 = 43.9 ± 4.9 %, GF109203X = 43.2 ± 6.9 %, KN93 = 39.6 ± 6.4 %, H89 = 40.3 ± 5.5 %; test path: BAPTA = 40.1 ± 5.0 %, thapsigargin = 49.1 ± 5.7 %, heparin = 40.6 ± 5.6 %, 2APB = 41.6 ± 5.2 %, U73122 = 42.6 ± 3.8 %, GF109203X = 39.5 ± 8.0 %, KN93 = 68.0 ± 7.2 %, H89 = 71.1 ± 6.5 %). Horizontal lines indicate the average value in the control path in absence of pharmacological agents; * indicates $P < 0.05$. Summary data expressed as average ± sem. BAPTA, 10 mM, n = 6; thapsigargin, 5 μM, n = 7; heparin, 10 mg/mL, n = 6; 2APB, 100 μM, n = 7; GF109203X, 1 μM, n = 8; KN93, 10 μM, n = 7

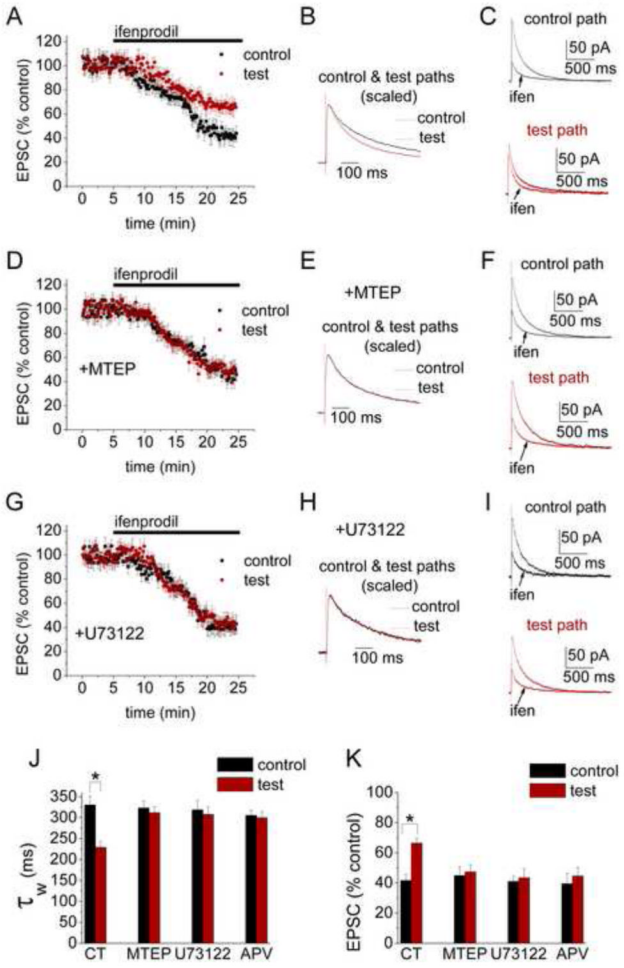

Figure 4. The activity-dependent switch in NR2 subunit composition induced in mouse hippocampal slices

(A) Summary data of NMDA EPSC peak amplitude vs. time plot for two independent pathways onto the same cell performed in mouse hippocampal slice (prepared from P5-7 mouse). In one pathway (test; red) the induction protocol (100 Hz tetanus for 6 s) was applied prior to the start of whole-cell recording, ifenprodil (5 μM) was bath-applied at the time indicated (n = 9). (B) NMDA EPSCs from example experiments for the test and control pathways taken from the experiments in A. (C) NMDA EPSCs from an example experiment showing changes in the ifenprodil sensitivity in the control and test paths after application of the induction protocol. (D-F) As for A-C, but in the presence of MTEP (10 μM; n = 8). (G-I) As for A-C, but in the presence of U73122 (5 μM; n = 7). (J) Summary graph showing the average values for the weighted time constant (τ_w) in the control and test paths, before and after the induction protocol in control (CT) and in the presence of the different antagonists (control path: CT = 330 ± 20 ms, MTEP = 323 ± 17 ms, U73122 = 318 ± 23 ms, APV = 305 ± 12 ms; test path: CT = 229 ± 14 ms, MTEP = 312 ± 15 ms, U73122 = 307 ± 18 ms, APV = 300 ± 15 ms). (K) Summary graph for EPSC amplitude in the presence of ifenprodil expressed as percentage of pre-ifenprodil amplitude (control path: CT = 41.7 ± 4.1 %, MTEP = 44.9 ± 5.8 %, U73122 = 41.0 ± 3.5 %, APV = 39.5 ± 6.9 %; test path: CT = 66.4 ± 3.3 %, MTEP = 47.4 ± 4.6 %, U73122 = 43.4 ± 6.2 %, APV = 44.6 ± 5.8 %).

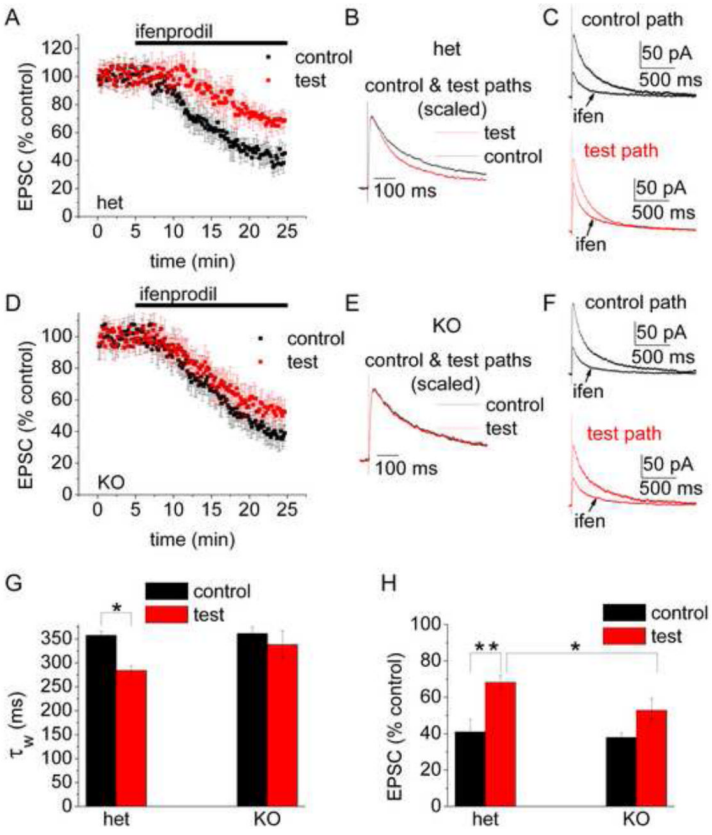

Figure 5. Impaired activity-dependent NR2 subunit switch in the mGluR5 knock-out mice

(A) Summary data of NMDA EPSC peak amplitude vs. time plot for two independent pathways onto the same cell performed in hippocampal slice from mGluR5 heterozygous (het) mouse (P5-7). In one pathway (test; red) the induction protocol (100 Hz tetanus for 6 s) was applied prior to the start of whole-cell recording, ifenprodil (5 μM) was bath-applied at the time indicated (n = 16 mice). (B) NMDA EPSCs from example experiments for the test and control pathways taken from the experiments in A. (C) NMDA EPSCs from an example experiment showing changes in the ifenprodil sensitivity in the control and test paths after application of the induction protocol. (D-F) As for A-C, but for mGluR5 knock-out (KO) (n = 9 mice). (G) Summary graph showing the average values for the weighted time constant (τ_w) in the control and test paths, before and after the induction protocol in mGluR5 heterozygous mice (het) and mGluR5 knock-out (KO) (control path: het = 358 ± 8 ms, KO = 361 ± 14 ms; test path: het = 284 ± 10 ms, KO = 338 ± 29 ms). (H) Summary graph for EPSC amplitude in the presence of ifenprodil expressed as percentage of pre-ifenprodil amplitude (control path: het = 41.0 ± 6.9 %, KO = 37.9 ± 2.6 %; test path: het = 68.2 ± 3.7 %, KO = 52.8 ± 6.5 %).

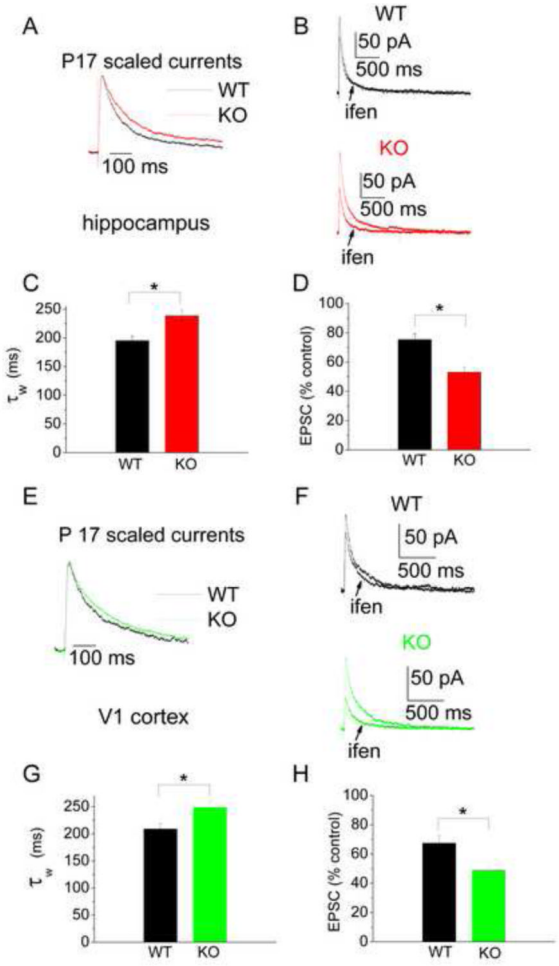

Figure 6. Impaired developmental switch in NR2 subunit composition in hippocampus and primary visual cortex ofmGluR5 knock-out mice

(A) Scaled NMDA EPSCs from hippocampal example experiments taken from wild type (WT, black) and mGluR5 knock-out (KO, red). (B) NMDA EPSCs from hippocampal example experiments taken showing ifenprodil sensitivity. (C) Summary graph showing the average values for the weighted time constant (τ_w) in wild type (WT) and mGluR5 knock-out (KO) at P15-18 (WT = 195 ± 8 ms, KO = 238 ± 10 ms). (D) Summary graph for EPSC amplitude in the presence of ifenprodil expressed as percentage of pre-ifenprodil amplitude for wild type (WT) and mGluR5 knock-out (KO) at P15-18 (WT = 75.4 ± 4.0 %, KO = 53.0 ± 3.6 %). n = 8 mice (E-H) As for A-D, but for layer 4 inputs onto layer 2/3 pyramidal neurons in primary visual cortex from P15-19 mice (decay kinetics: WT = 209 ± 9 ms, KO = 249 ± 13 ms; ifenprodil sensitivity: WT = 67.4 ± 5.3 %, KO = 48.7 ± 3.4 %). n = 8 mice. *p < 0.05

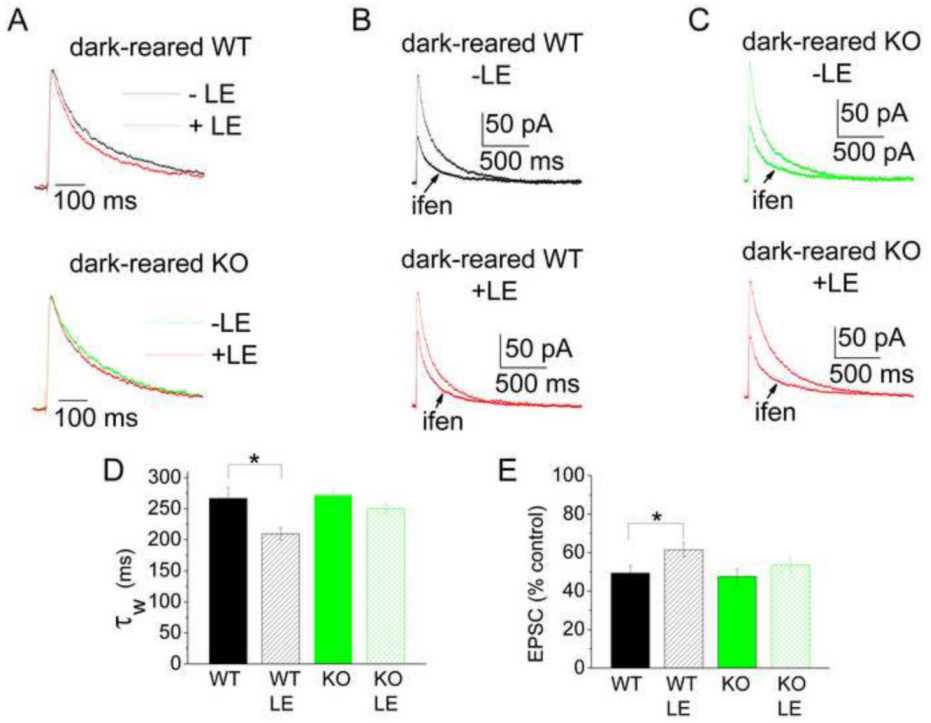

Figure 7. Impaired sensory-experience switch in the NR2 subunit composition in mGluR5 knock-out mice

(A) Scaled NMDA EPSCs from dark-reared wild type (WT, top) or mGluR5 knock out mice (KO, bottom) without (black trace for WT and green trace for KO) or with (red traces) 2.5 hours light experience (LE). (B) Example traces for ifenprodil sensitivity in dark-reared wild type mice (WT) without light experience (−LE, top) or with light experience (+LE, bottom). (C) Example traces for ifenprodil sensitivity in dark-reared mGluR5 knock-out mice (KO) without light experience (−LE, top) or with light experience (+LE, bottom). (D) Summary graph showing the average values for the weighted time constant (τ_w) in wild type (WT) and mGluR5 knock-out (KO) with or without LE (WT = 267 ± 18 ms, WT LE = 210 ± 9ms, KO = 271 ± 10 ms, KO LE = 250 ± 8 ms). (E) Summary graph for NMDAR EPSC amplitude in the presence of ifenprodil expressed as percentage of pre-ifenprodil amplitude for wild type (WT) and mGluR5 knock-out (KO) with or without LE (WT = 49.4 ± 3.8 %, WT LE = 61.5 ± 3.7 %, KO = 47.6 ± 3.9 %, KO LE = 53.5 ± 3.6 %). n = 10 animals, *p < 0.05

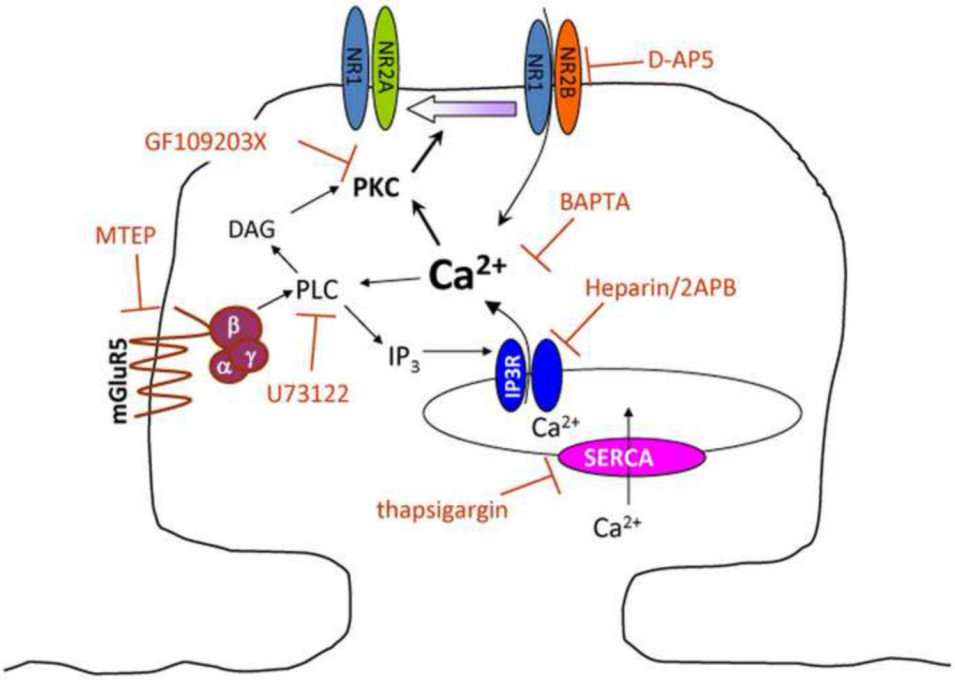

Figure 8. Mechanism for the activity-dependent switch in NR2 subunit composition

Schematic of a dendritic spine showing the receptors and signaling pathways involved in the activity-dependent NR2 subunit switch. The pharmacological agents used to block the activity-dependent switch are also shown.